



Original Article

The IRF1/GBP5 axis promotes osteoarthritis progression by activating chondrocyte pyroptosis

Hao Tang^{a,1}, Xiaoshan Gong^{a,1}, Jingjin Dai^a, Jun Gu^a, Zicai Dong^a, Yuan Xu^b, Zhaoyang Hu^c, Chunrong Zhao^a, Jiezhong Deng^d, Shiwu Dong^{a,e,*}^a Department of Biomedical Materials Science, College of Biomedical Engineering, Third Military Medical University, Chongqing, 400038, China^b Department of Orthopedics, Xinqiao Hospital, Third Military Medical University, Chongqing, 400037, China^c Department of Burn and Plastic, Joint Logistic Support Force 921th Hospital, Changsha, 410153, China^d Department of Orthopedics, Southwest Hospital, Third Military Medical University, Chongqing, 400038, China^e State Key Laboratory of Trauma and Chemical Poisoning, Army Medical University, Chongqing, 400038, China

ARTICLE INFO

Keywords:

ECM
GBP5
IRF1
NLRP3 inflammasome
OA
Pyroptosis

ABSTRACT

Background: Osteoarthritis (OA) is a chronic degenerative joint disease that primarily affects middle-aged and elderly individuals. The decline in chondrocyte function plays a crucial role in the development of OA. Inflammasome-mediated chondrocyte pyroptosis is implicated in matrix degradation and cartilage degeneration in OA patients. Guanylate binding protein 5 (GBP5), a member of the GTPase family induced by Interferon- γ (IFN- γ), significantly influences cellular inflammatory responses, including intracellular inflammasome activation and cytokine release. However, the role of GBP5 in chondrocyte pyroptosis and OA progression remains unclear.

Methods: In this study, we used tumor necrosis factor- α (TNF- α) to induce inflammation and created an OA mouse model with surgically-induced destabilization of the medial meniscus (DMM). We isolated and cultured primary chondrocytes from the knee joints of suckling C57 mice. TNF- α -stimulated primary chondrocytes served as an in vitro model for OA and underwent RNA sequencing. Chondrocytes were transfected with GBP5-overexpression plasmids and small interfering RNA and were subsequently treated with TNF- α . We assessed the expression of cartilage matrix components (COL2A1 and aggrecan), catabolic factors (MMP9 and MMP13), and NLRP3 inflammasome pathway genes (NLRP3, Caspase1, GSDMD, Pro-IL-1 β , and Pro-Caspase1) using RT-qPCR and Western blotting. We analyzed the expression of GBP5, NLRP3, and Caspase1 in the cartilage of DMM-induced post-traumatic OA mice and human OA patients. Immunohistochemistry (IHC) was used to detect the expression of GBP5, NLRP3 and GSDMD in cartilage specimens from OA patients and mouse DMM models. Chondrocyte pyroptosis was assessed using flow cytometry, and the levels of interleukin-1 β (IL-1 β) and interleukin-18 (IL-18) were measured with ELISA. We conducted double luciferase reporter gene and chromatin immunoprecipitation (ChIP) assays to confirm the relationship between IRF1 and GBP5.

Results: GBP5 expression increased in TNF- α -induced chondrocytes, as revealed by RNA sequencing. GBP5 inhibited COL2A1 and aggrecan expression while promoting the expression of MMP9, MMP13, NLRP3, Caspase1, GSDMD, Pro-IL-1 β , and Pro-Caspase1. GBP5 expression also increased in the cartilage of DMM-induced post-traumatic OA mice and human OA patients. Knockout of GBP5 reduced chondrocyte injury in OA mice. GBP5 promoted chondrocyte pyroptosis and the production of IL-1 β and IL-18. Additionally, we found that IRF1 bound

Abbreviations: OA, osteoarthritis; GBP5, guanylate binding protein 5; IRF1, interferon regulatory factor 1; IL-1 β , interleukin-1 β ; IL-18, interleukin-18; TNF- α , tumor necrosis factor- α ; MMPs, matrix metalloproteinases; ADAMTS4, a disintegrin and metalloproteinase with thrombospondin motifs 4; ADAMTS5, a disintegrin and metalloproteinase with thrombospondin motifs 5; ECM, extracellular matrix; COL2A1, type II collagen; GSDMD, gasdermin D; DMM, destabilization of the medial meniscus; MCCs, mouse chondrocytes; MMP9, matrix metalloproteinase 9; MMP13, matrix metalloproteinase 13; NLRP3, NOD-like receptor thermal protein domain associated protein 3; IHC, immunohistochemistry; CHIP, chromatin Immunoprecipitation; DEPs, differentially expressed proteins; NC, negative control; LPS, lipopolysaccharide.

* Corresponding author. Department of Biomedical Materials Science, College of Biomedical Engineering, Third Military Medical University, Chongqing, 400038, China.

E-mail address: dongshiwu@tmmu.edu.cn (S. Dong).

¹ These authors contributed equally to this work.

<https://doi.org/10.1016/j.jot.2023.11.005>

Received 7 June 2023; Received in revised form 2 October 2023; Accepted 11 November 2023

2214-031X/© 2023 The Authors. Published by Elsevier B.V. on behalf of Chinese Speaking Orthopaedic Society. This is an open access article under the CC BY-NC-ND license (<http://creativecommons.org/licenses/by-nc-nd/4.0/>).

to the promoter region of GBP5, enhancing its expression. After co-transfected with ad-IRF1 and siGBP5, the expression of pyroptosis-related genes was significantly decreased compared with ad-IRF1 group.

Conclusions: The IRF1/GBP5 axis enhances extracellular matrix (ECM) degradation and promotes pyroptosis during OA development, through the NLRP3 inflammasome signaling pathway.

The translational potential of this article: This study underscores the significance of the IRF1/GBP5 axis in NLRP3 inflammasome-mediated chondrocyte pyroptosis and osteoarthritic chondrocyte injury. Modulating IRF1 and GBP5 expression could serve as a novel therapeutic target for OA.

1. Introduction

Osteoarthritis (OA) is a chronic degenerative joint disease that predominantly affects middle-aged and elderly individuals. Its prevalence increases with age, impacting approximately 7 % of the global population [1]. While OA leads to various pathological changes such as joint space narrowing, osteophyte formation, and synovitis, the degradation of articular cartilage is its hallmark feature [2,3]. Inflammation plays a pivotal role in cartilage loss and OA symptomatology. Overproduction of inflammatory cytokines, including interleukin-1 β (IL-1 β) and tumor necrosis factor- α (TNF- α) [4], stimulates chondrocytes to secrete stroma-degrading enzymes like matrix metalloproteinases (MMPs) and a disintegrin and metalloproteinase with thrombospondin motifs 4 and 5 (ADAMTS4 and ADAMTS5), contributing to cartilage matrix degradation and OA onset [5,6]. Chondrocytes, the sole cell type in articular cartilage, synthesize an extracellular matrix (ECM) primarily composed of aggrecan and type II collagen (COL2A1) to maintain normal joint cartilage morphology, structure, and function [7]. Altered chondrocyte status and function can drive OA progression.

Excessive inflammation leads to chondrocyte pyroptosis, the principal cause of matrix degradation and cartilage degeneration in OA patients. Pyroptosis, a pro-inflammatory programmed cell death process, is triggered by inflammasomes. Caspase1 or caspase11/4/5 activation characterizes pyroptosis, leading to gasdermin D (GSDMD) cleavage, cell membrane rupture, and release of cellular contents [8,9]. Released inflammatory factors recruit more immune cells, amplifying the inflammatory response [10]. Pyroptosis has been implicated in common inflammation-related diseases such as cardiovascular diseases [11], periodontal diseases [12], and liver diseases [13], and recent studies have linked pyroptosis-related pathways to OA [14–16]. Thus, understanding the molecular mechanisms of chondrocyte pyroptosis and ECM degradation in OA can provide valuable insights into disease pathogenesis and potential strategies for effective OA prevention, amelioration, or reversal.

Guanylate binding protein 5 (GBP5), a member of the GTPase family induced by Interferon- γ (IFN- γ), participates in cellular inflammatory responses, including intracellular inflammasome activation and cytokine release [17]. For instance, GBP5 promotes the assembly of the mammalian NLRP3 inflammasome and exacerbates transcriptional enhancement-mediated sepsis-associated liver injury through NLRP3 inflammasome activation [18,19]. Recent research has confirmed the pro-inflammatory role of GBP5 [20,21]. However, the impact of GBP5 on OA, and its underlying mechanism, remains unexplored.

This study conducts *in vivo* and *in vitro* experiments to elucidate GBP5's role in OA progression and its molecular mechanisms in promoting chondrocyte pyroptosis. We identify IRF1 as an upstream transcription factor that enhances GBP5 expression by binding to its promoter. The IRF1/GBP5 axis activates chondrocyte pyroptosis, driving cartilage matrix degradation and OA progression.

2. Materials and methods

2.1. Clinical specimens

Human cartilage samples were collected from patients undergoing total knee arthroplasty after obtaining informed consent and approval

from the Army Medical University Xinqiao Hospital (Approval number: 2022-495-01). Cartilage specimens were obtained from patients who had unilateral or bilateral joint replacement due to trauma. The intact parts of the cartilage specimens were selected for the Intact group, and all patients in this group were under 70 years of age. In contrast, cartilage specimens were obtained from patients aged 75–80 years who had undergone bilateral knee replacement due to OA for the OA group. All experiments were conducted in accordance with relevant ethical guidelines and approved research protocols.

2.2. Animals

All animal experiments were approved by the Laboratory Animal Welfare and Ethics Committee of the Third Military Medical University (AMUWEC20226250). Following the guidelines outlined in the Third Military Medical University Sciences Guide for Laboratory Animals, mice were group-housed at 23–25 °C with a 12 h/12 h light/dark cycle. They had free access to water and standard laboratory pellets.

Male mice (12 months old) underwent surgical procedures on their right knees, either via destabilization of the medial meniscus (DMM) surgery or sham surgery, to induce OA. In DMM surgery, the joint capsule was opened following anesthesia, and the medial meniscus tibial ligament was cut to destabilize the meniscus without harming other tissues. In the sham surgery, the joint capsule was opened in the same manner, but no further damage was induced. Samples were collected eight weeks after DMM surgery. To knock down GBP5 expression, C57BL/6 J mice received intra-articular injections of GBP5 siRNA or a negative control (5 nmol/injection) twice a week for three weeks after DMM surgery. Samples were collected one week after the last injection.

2.3. Isolation and culture of chondrocytes

Chondrocytes were isolated from C57BL/6 mice (both male and female) at five days old, obtained from the Laboratory Animals Center of the Army Medical University. Following the protocols provided in the Army Medical University Sciences Guide for Laboratory Animals, primary mouse chondrocytes (MCCs) were collected from cartilage fragments dissected from the tibial plateau in aseptic conditions. Articular cartilage was cut into small pieces and digested with 0.25 % trypsin at 37 °C for 30 min in a culture dish (NEST Biotechnology, Wuxi, China). After triple washing with phosphate-buffered saline (PBS, Gibco, Waltham, MA, USA), the pieces were further digested with 0.05 % collagenase IV (BBI Solutions, Cardiff, UK) at 37 °C for 6 h. The resulting cell suspension was filtered through a 70 μ m cell strainer and centrifuged at 1000 rpm for 5 min to collect primary chondrocytes. These cells were cultured in Dulbecco's modified eagle medium (DMEM, Gibco) supplemented with 100 U/mL penicillin (Sigma-Aldrich, St. Louis, MO, USA), 100 g/mL streptomycin sulfate (Sigma-Aldrich), and 10 % fetal bovine serum (FBS, Gibco) at 37 °C in a 5 % CO₂ humidified incubator. Primary human chondrocytes purchased from Biospec, China. Experiments were conducted using chondrocytes in the second passage (P2).

2.4. Sequencing of mRNA and data analysis

Total RNA was extracted using Trizol (Life Technologies Corporation) and further treated with DNase to remove genomic DNA

contamination. mRNA was isolated using the mRNA Magnetic Isolation Module (New England Biolabs, Ipswich, MA, USA), and this isolated mRNA was used to prepare RNA-Seq libraries with the Ultra Directional RNA Library Prep Kit (New England Biolabs). The library was sequenced in paired-end 2 × 150 mode. Gene expression levels were estimated using FPKM (fragments per kilobase of exon per million fragments mapped) via StringTie [22]. Genes with adjusted P-values below 0.05 were used for subsequent analyses. The gene annotation file was sourced from Ensembl genome browser 90 databases (<http://www.ensembl.org/index.html>). Functional enrichment analyses (GO and KEGG) were conducted using ClusterProfiler.

2.5. Transfection

Transfection procedures followed manufacturer protocols and involved small-interfering RNA (siRNA) or plasmids. MCCs were adjusted to a concentration of 2.5×10^5 cells/mL. In six-well plates, 2 mL of cell suspension was seeded and incubated overnight at 37 °C with 5 % CO₂. Subsequently, 50 nM siRNA or 5 µg of plasmids were added to 125 µL of Opti-MEM™. Additionally, 5 µL of Lipofectamine 3000 (Invitrogen, San Diego, CA, USA) was mixed with 125 µL of Opti-MEM™ and incubated at 25 °C for 5 min. The solution containing siRNA or plasmid was then combined with the solution containing Lipofectamine 3000 and gently mixed for 15 min at room temperature. The siRNA or plasmid/liposome 3000 complex was added to six-well plates at 250 µL per well and mixed gently. After 48 h of transfection, the complex was removed and replaced with a fresh medium. Cells were subsequently treated with 20 µg/mL of TNF-α for 24 h and collected for further analysis. Western blotting and qPCR assays were performed to assess silencing or overexpression efficiency.

2.6. Real-time quantitative PCR

Total RNA was extracted using RNAiso Plus reagent (Takara, Kusatsu, Shiga, Japan). The first-strand cDNAs were prepared from 1 mg of total RNA using the PrimeScript™ RT reagent Kit with gDNA Eraser (Takara) following the manufacturer's instructions. The primers for RT-qPCR are listed in Table S1.

2.7. Western blotting

Cells were lysed in cell lysis buffer (Thermo Fisher Scientific, Pittsburgh, USA). The protein concentration in the cell homogenate was determined using a bicinchoninic acid (BCA) assay kit (Beyotime, Shanghai, China). SDS-PAGE separated the proteins (30 µg), which were subsequently transferred onto polyvinylidene fluoride (PVDF) membranes (Biorbyt, Cambridge, UK). After blocking with 5 % skim milk for 2 h, the membranes were incubated overnight at 4 °C with rabbit antibodies against GBP5 (1:2000, 13,220-1-AP, Proteintech, Wuhan, Hebei, China), IRF1 (1:1000, 8478s, CST, Boston, USA), MMP9 (1:1000, ab228402, Abcam, MA, USA), MMP13 (1:1000, bs10581 R, Bioss, Boston, MA, USA), COL2A1 (1:1000, ab34712, Abcam), aggrecan (1:1000, AF6126, Beyotime), Sox9 (1:1000, BS1597, Bioworld, Nanjing, Jiangsu, China), NLRP3 (1:1000, bs1001 R, Bioss), Caspase1 (1:1000, BS5641, Bioworld), GSDMD (1:1000, ab219800, Abcam), Pro-IL-1β (1:1000, ab216995, Abcam), Pro-Caspase1 (1:1000, ab179515, Abcam), and GAPDH (1:1000, 5174s, CST, Boston, USA). Subsequently, the membranes were incubated with secondary antibodies (1:20,000, BS13278, Bioworld) at room temperature for 1.5 h. After washing the membranes in TBST, chemiluminescent signals were detected using a Bio-Rad Molecular Imager ChemiDoc™ XRS + system (Bio-Rad, Hercules, CA, USA), with GAPDH serving as the loading control.

2.8. Flow cytometry analysis of cell pyroptosis

To assess cell pyroptosis, a double staining of propidium iodide (PI)

and Caspase1 was performed followed by flow cytometry analysis. Initially, cells were collected and washed twice with PBS. Subsequently, cells were resuspended in 500 µL of binding buffer at a concentration of 1×10^6 cells/mL. They were then stained with 5 µL of anti-Caspase1 antibody conjugate and 5 µL of propidium iodide solution (PI) (C2015M, Beyotime). After a 10-min incubation in the dark at room temperature, the stained cells were analyzed using flow cytometry.

2.9. Cytokine measurements

Supernatants from six-well plates transfected with siRNAs or plasmids and stimulated with TNF-α were harvested. Cytokines were quantified using mouse IL-1β and interleukin-18 (IL-18) ELISA kits (Multisciences, Hangzhou, China) following the manufacturer's instructions.

2.10. Histology and immunohistochemical assay

Tissues were fixed in 4 % paraformaldehyde, decalcified with EDTA decalcifying solution (pH 7.2), and then embedded in paraffin. Sections were prepared and stained with safranin O/fast green.

For immunohistochemistry (IHC) staining, sections were heated at 95 °C for 15 min, treated with 3 % H₂O₂ and 0.5 % Triton X-100, and blocked using 10 % bovine serum albumin for 1 h at room temperature. Subsequently, sections were incubated with primary antibodies (GBP5, 1:100, 13220-1-AP, Proteintech; NLRP3, 1:100, bs10021 R, Bioss; Caspase1, 1:100, BS65650, Bioworld) overnight at 4 °C. Following primary antibody incubation, sections were incubated with biotinylated secondary antibodies, counterstained with hematoxylin, and visualized using DAB solution for IHC.

2.11. Dual-luciferase reporter assay

To investigate whether IRF1 directly targets the GBP5 promoter region, wild-type (WT) and mutant (MUT, mutated at a specific site) sequences of the GBP5 promoter region were ligated into pGL3-basic to construct luciferase reporter plasmids (KnoriGene, Chongqing, China). Subsequently, 293 T cells were transfected with DNA vectors containing wild-type and mutant plasmids, along with plasmids overexpressing IRF1. A vector containing the Renilla luciferase gene was introduced as an internal reference. After 48 h of transfection, the cells were seeded in 96-well plates and incubated overnight at 37 °C with 5 % CO₂. Luciferase expression levels were measured using the Dual-Luciferase Reporter Assay System kit (Promega, WI, USA), and both firefly and Renilla luciferin expression levels were measured using a multi-function microplate reader. Experiments were repeated six times.

2.12. Chromatin immunoprecipitation (ChIP) assay

The ChIP assay was conducted in mouse chondrocytes using a ChIP Assay Kit (CST). Briefly, mouse chondrocytes were cross-linked with 1 % formaldehyde at 37 °C for 15 min, washed, and then harvested in SDS lysis buffer. The DNA was sheared by sonication to fragment it. Sonicated cell lysates were precipitated with 1 µg of IRF1 antibody (8478s, CST) or non-specific IgG (Thermo Fisher Scientific) and protein-A/G agarose beads. From the cross-linked DNA/protein complexes, the DNA was purified and used for polymerase chain reaction (PCR, Takara, Japan). The primers were designed from 100 bp upstream to 100 bp downstream of the binding site and were 5'- AAATATACCCCTCGTCAAAGG-3' (forward) and 5'- CAGAAGGCTTGAATGCTACTGA- 3' (reverse).

2.13. Statistical analysis

The data were expressed as the mean ± standard error of the mean (SEM). The statistical difference between groups was analyzed by two-

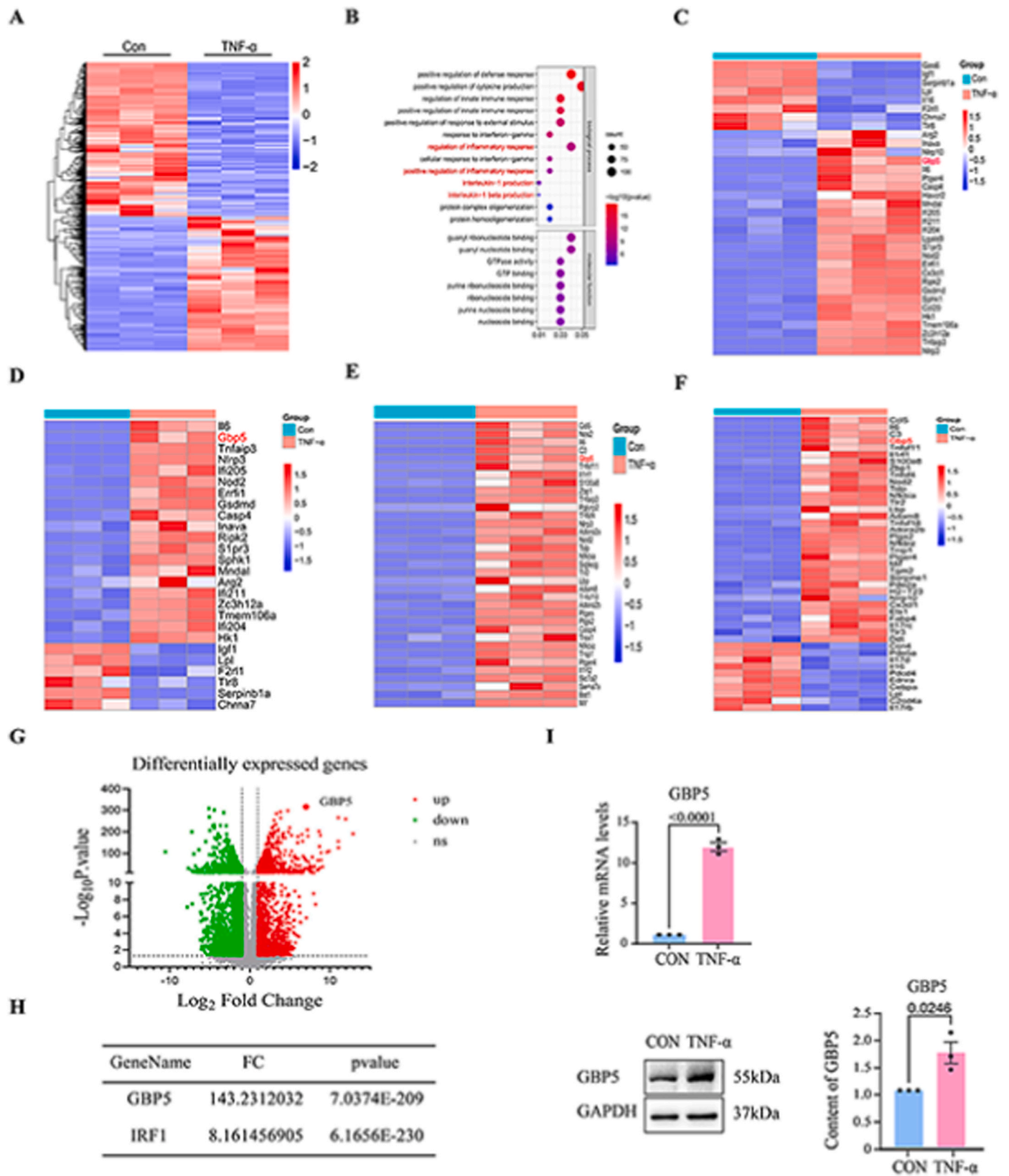


Figure 1. GBP5 was upregulated in chondrocytes of OA models in vitro (A) A heat map of differentially expressed proteins (DEPs) in TNF- α -treated chondrocytes, as determined from the results of the RNA-seq analysis (B) The GO analysis of DEPs (C–F) The sequencing of DEPs in the signaling pathways was highly associated with inflammatory responses (G) A volcano map of DEPs (H) The differences among related genes were determined by RNA-seq. (I) The level of expression of the GBP5 gene and protein after treatment with TNF- α was determined by RT-qPCR and Western blotting analyses. The data were expressed as the mean \pm SEM and analyzed by two-tailed t-tests.

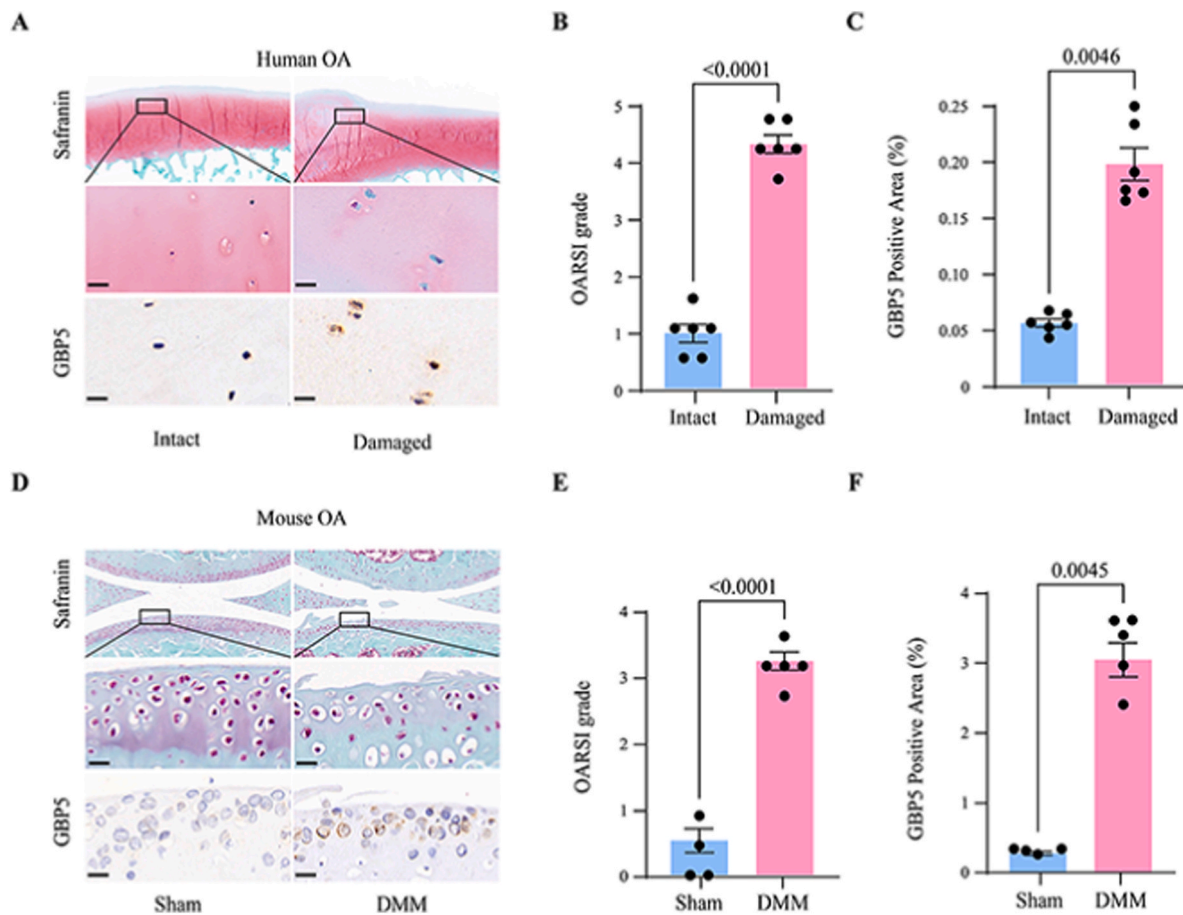


Figure 2. GBP5 was upregulated in osteoarthritic chondrocytes in vivo (A) Safranin-O staining and immunostaining for GBP5 in the cartilage tissue of humans with OA (n = 6) (B) The OARSI grade of cartilage tissue of humans (C) The expression of GBP5 in the cartilage tissue of humans (D) Safranin-O staining and immunostaining for GBP5 in the cartilage tissue of sham-operated or DMM-operated mice (E) The OARSI grade of cartilage tissue of mice (F) The expression of GBP5 in the cartilage tissue of mice. The data were expressed as the mean ± SEM and analyzed by two-tailed t-tests, n = 6. Scale bar = 25 μm.

sample t-tests using the GraphPad Prism 9 software (GraphPad Software Inc., San Diego, CA, USA). The statistical difference among multiple groups was analyzed by one-way analysis of variance (ANOVA). All differences among or between groups were considered statistically significant at $p < 0.05$. The data were assessed from at least three independent in vitro experiments.

3. Results

3.1. GBP5 is upregulated in chondrocytes induced by TNF- α and in the osteoarthritic cartilage

Inflammation is a significant pathogenic factor in OA, and the TNF- α -induced chondrocyte model is widely recognized for studying inflammatory injury. The study assessed changes in gene and protein expression in chondrocytes exposed to TNF- α -induced inflammation (Fig. S1A). To investigate the mechanisms underlying OA development, RNA sequencing was performed using a TNF- α -induced inflammatory model in primary chondrocytes. A heatmap of differentially expressed proteins (DEPs) is presented in Fig. 1A. Through DEP enrichment, 21 signaling pathways associated with the inflammatory response were identified, and four signaling pathways highly correlated with inflammation were selected for DEP sequencing, including regulation of inflammatory response, positive regulation of inflammatory response, interleukin-1 production and interleukin1 β production (Fig. 1B–F). GBP5 was found to be the common gene at the top of the DEP list. The volcano plot of DEPs is displayed in Fig. 1G, and GBP5's expression in

DEPs is shown in Fig. 1H. RT-qPCR and Western blotting demonstrated significantly higher GBP5 gene and protein expression in chondrocytes stimulated by TNF- α (Fig. 1I). GBP5 expression was also significantly elevated in cartilage from OA patients (Fig. 2A–C) and cartilage from DMM-induced post-traumatic OA mice (Fig. 2D–F). These findings suggest that GBP5 is significantly upregulated in OA.

3.2. GBP5 promotes the expression of MMP9 and MMP13 in chondrocytes and inhibits the expression of COL2A1 and aggrecan

Given the significant upregulation of GBP5 in TNF- α -induced chondrocyte inflammation, DMM-induced OA mouse models, and human OA specimens, the study further explored GBP5's role. GBP5-overexpressing plasmids (ad-GBP5) and GBP5 siRNA (siGBP5) were used to investigate its effects. The transfection efficiency of siGBP5 and ad-GBP5 in chondrocytes was confirmed by qRT-PCR and Western blotting (Fig. S1B). First, primary chondrocytes were transfected with ad-GBP5 and an empty vector (Vector), followed by TNF- α stimulation for 24 h, with PBS serving as the negative control. The results of RT-qPCR and Western blotting revealed significantly higher expression of MMP9 and MMP13 genes and proteins and significantly lower expression of COL2A1 and aggrecan genes and proteins in the ad-GBP5 group compared to the Vector group when TNF- α or PBS was used to stimulate the cells (Fig. 3A and C). Next, primary chondrocytes were transfected with GBP5 siRNA (siGBP5) and a non-targeting siRNA (siNC), followed by TNF- α stimulation under the same conditions, with PBS as the negative control. RT-qPCR and Western blotting results demonstrated significantly lower

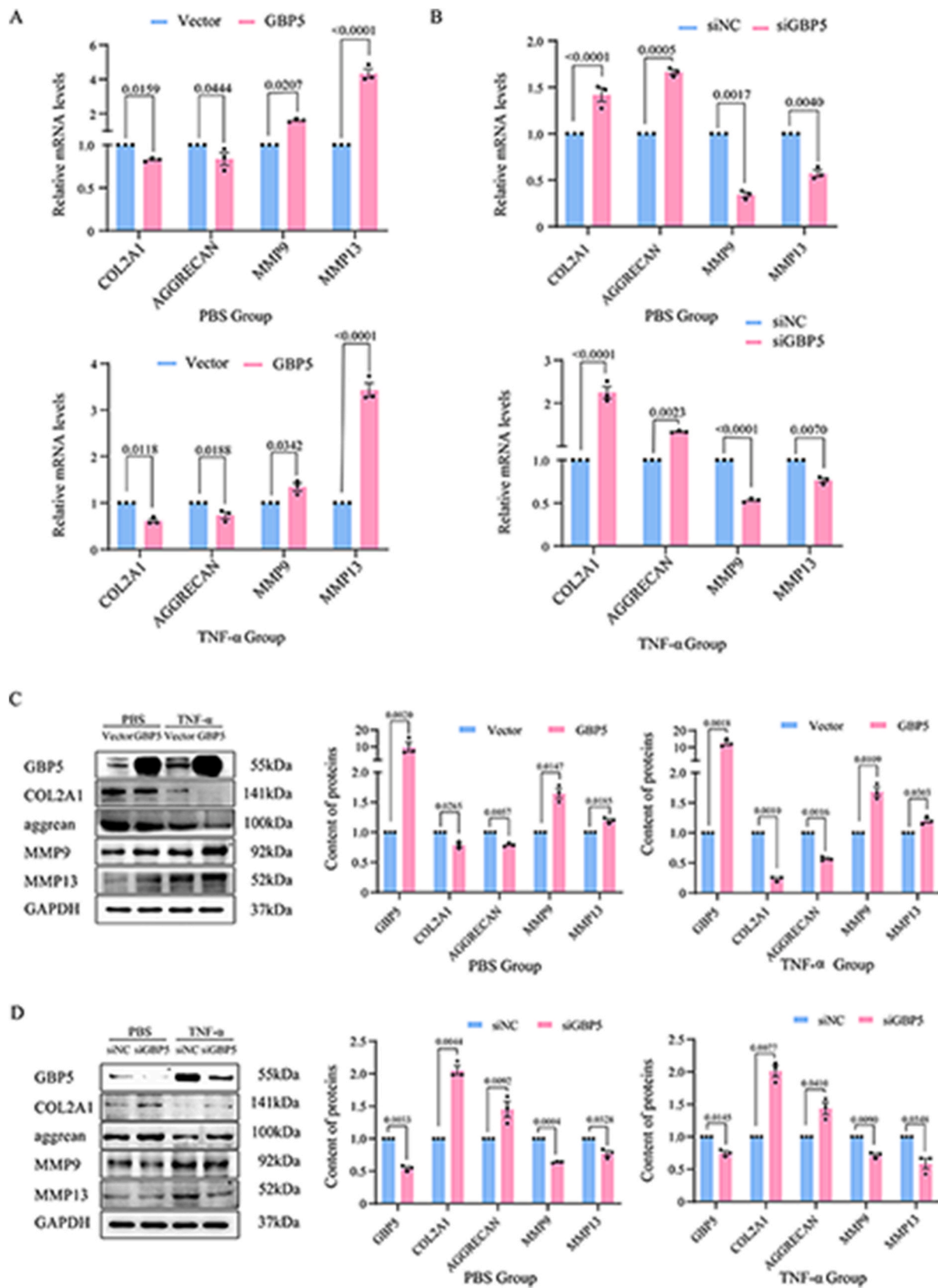


Figure 3. GBP5 regulated the synthesis and degradation of ECM in the progression of OA (A) The level of expression of the COL2A1, aggrecan, MMP9, and MMP13 genes after the overexpression of GBP5 was determined by RT-qPCR (B) The level of expression of the COL2A1, aggrecan, MMP9, and MMP13 genes after knocking down GBP5 was determined by RT-qPCR analysis (C) The level of expression of the COL2A1, aggrecan, MMP9, and MMP13 proteins after the overexpression of GBP5 was determined by Western blotting (D) The level of expression of the COL2A1, aggrecan, MMP9, and MMP13 proteins after knocking down GBP5 was determined by Western blotting. Two-tailed t-tests were performed to analyze the data on the PBS and TNF-α groups. The data were expressed as the mean ± SEM.

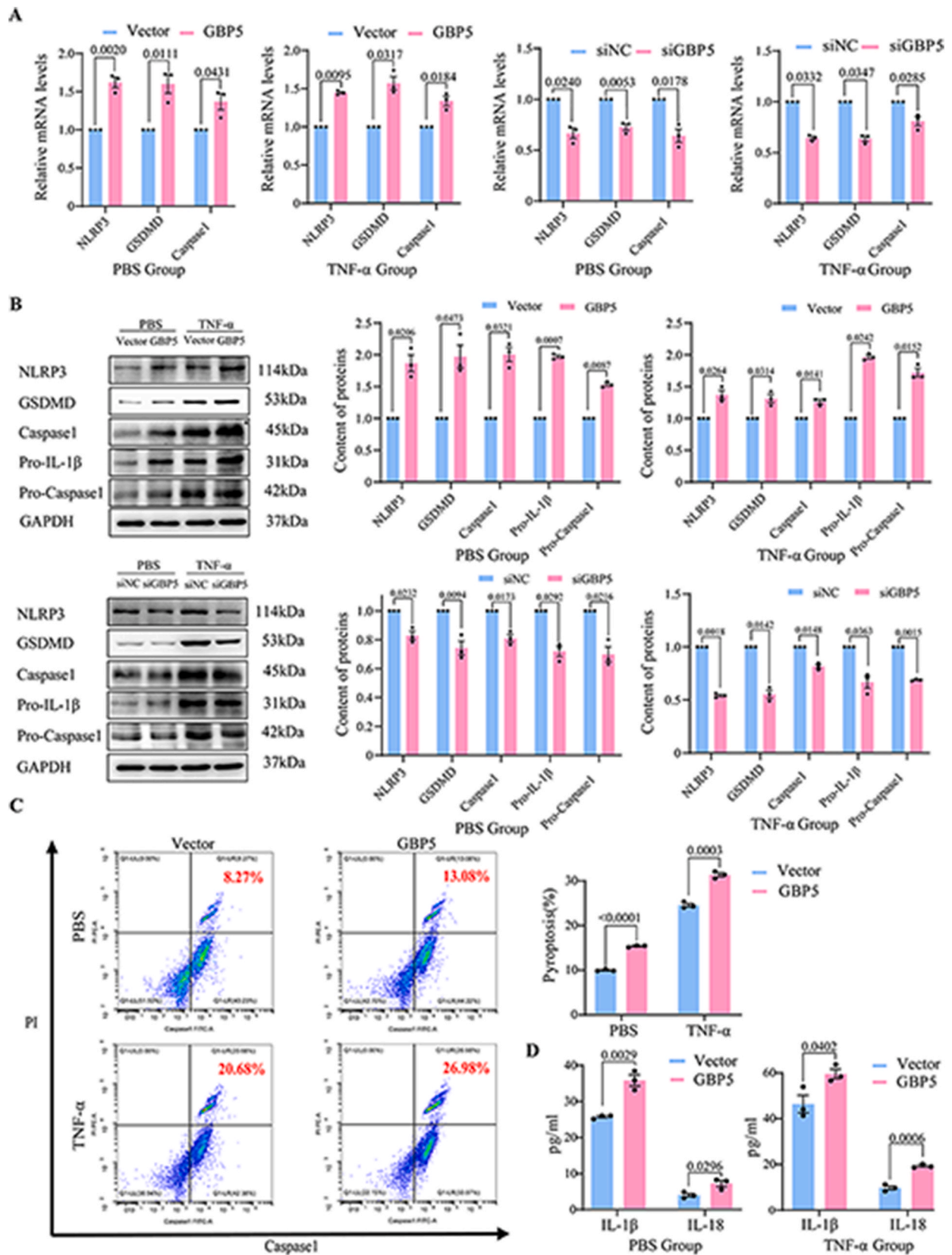
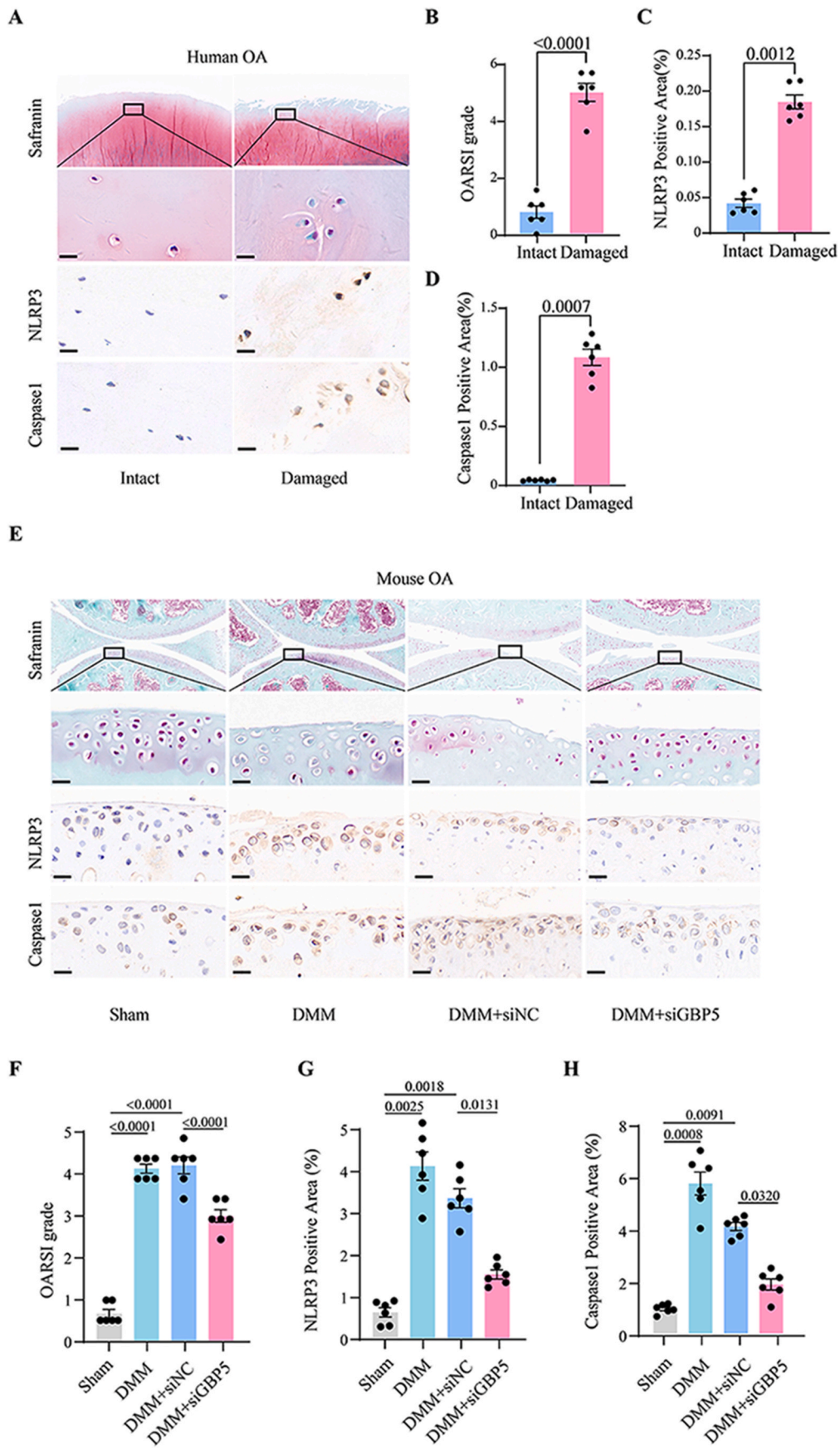


Figure 4. GBP5 induced chondrocyte pyroptosis through the NLRP3 inflammasome pathway (A) The level of expression of the NLRP3, Caspase1, and GSDMD genes was determined by RT-qPCR (B) The level of expression of the NLRP3, Caspase1, and GSDMD proteins was determined by Western blotting (C) Cell pyroptosis was evaluated by flow cytometry (D) The levels of IL-1β and IL-18 in the supernatant were estimated by ELISA. Two-tailed t-tests were performed to analyze the data on the PBS and TNF-α groups. The data were expressed as the mean ± SEM.



(caption on next page)

Figure 5. Knockout of GBP5 decreased chondrocyte pyroptosis and reduced chondrocyte injury in OA mice (A) Safranin-O staining and immunostaining for NLRP3 and Caspase1 from the cartilage tissue of humans with OA (n = 6) (B) The OARSI grade of cartilage tissue of humans (C) Immunostaining was applied to detect the positive area of NLRP3 (D) Immunostaining was applied to detect the positive area of Caspase1 (E) Safranin-O staining and immunostaining were performed for the cartilage tissue of sham-operated, DMM-operated, DMM + siNC and DMM + siGBP5 mice (F) The OARSI grade of cartilage tissue of mice. The OARSI grade in the DMM + siGBP5 group decreased compared with the DMM + siNC group (G) Immunostaining was applied to detect the positive area of NLRP3. NLRP3 expression in the DMM + siGBP5 group decreased compared with the DMM + siNC group (H) Immunostaining was applied to detect the positive area of Caspase1. Caspase1 expression in the DMM + siGBP5 group decreased compared with the DMM + siNC group. The data were expressed as the mean \pm SEM and analyzed by two-tailed t-tests (B–D). The data were expressed as the mean \pm SEM and analyzed by one-way analysis of variance (F–H). Scale bar = 25 μ m, n = 6.

expression of MMP9 and MMP13 genes and proteins and significantly higher expression of COL2A1 and aggrecan genes and proteins in the siGBP5 group compared to the siNC group when TNF- α or PBS was used to stimulate the cells (Fig. 3B and D). These findings suggest that GBP5 is involved in ECM synthesis and degradation during OA progression.

3.3. GBP5 induces chondrocyte pyroptosis through the NLRP3 inflammasome pathway

The study identified the NLRP3 inflammasome as a transcriptional target of GBP5, capable of triggering pyroptosis. After TNF- α stimulation, the ad-GBP5 group exhibited significantly upregulated expression of the NLRP3 gene and protein compared to the Vector group, while the siGBP5 group displayed significantly downregulated expression compared to the siNC group. Moreover, cascade factors activated as a result of NLRP3 activation, such as GSDMD, Caspase1, pro-IL-1 β , and pro-IL-18, showed corresponding upregulation or downregulation alongside changes in NLRP3 levels (Fig. 4A and B). The same results were obtained when GBP5 was knocked down in primary human chondrocytes (Figs. S4C and D). These changes were observed even in the absence of TNF- α stimulation, suggesting that GBP5 induced NLRP3 inflammasome activation in chondrocytes. This led to the hypothesis that GBP5 might play a role in promoting chondrocyte pyroptosis in OA by activating the NLRP3 inflammasome. To validate this hypothesis, key indicators of pyroptosis, including Caspase1, IL-1 β , and IL-18, were assessed. Flow cytometry analysis demonstrated that GBP5 overexpression increased Caspase1 expression (Fig. 4C), while knocking out GBP5 decreased Caspase1 expression, regardless of whether TNF- α or PBS was added to chondrocytes (Fig. S2A).

ELISA results revealed that GBP5 overexpression in TNF- α -stimulated or PBS-treated chondrocytes led to increased secretion of IL-1 β and IL-18 (Fig. 4D), while GBP5 knockout reduced the production of IL-1 β and IL-18 (Fig. S2B). The same results were obtained when GBP5 was knocked down in primary human chondrocytes (Fig. S4B). Immunohistochemical staining of human osteoarthritic cartilage showed significantly higher expression of NLRP3 and Caspase1 (Fig. 5A–D). Additionally, in mice with GBP5 knockout, the expression of NLRP3 and Caspase1, as well as the OARSI grade, decreased compared to DMM-induced osteoarthritic mice (Fig. 5E–H and S1D). These findings collectively suggested that GBP5 acts as an upstream regulator of NLRP3-mediated inflammasome activation and that GBP5 induces chondrocyte pyroptosis through the NLRP3 inflammasome pathway. GBP5 knockout reduced chondrocyte pyroptosis and alleviated chondrocyte injury in OA mice.

3.4. IRF1 binds to the GBP5 promoter region and enhances its expression

Given the association between GBP5 and NLRP3 expression, the study sought to identify transcription factors that directly bind to the GBP5 promoter response elements in osteoarthritic chondrocytes. IRF1 was a potential candidate due to its ability to bind to specific DNA sequences in IFN- β promoters that mediate viral reactivity and its strong influence on inflammasome activation [23]. RNA sequencing revealed significantly higher IRF1 expression in TNF- α -stimulated primary chondrocytes compared to the control group (Fig. 1H). Therefore, IRF1 was hypothesized to regulate GBP5 expression in OA chondrocytes. Bioinformatics analysis using the JASPAR database (<https://jaspar.genereg.net>) predicted multiple binding sites for IRF1 in the GBP5 promoter region.

To confirm that IRF1 activates GBP5 transcription, primary chondrocytes were transfected with an IRF1-overexpression plasmid (ad-IRF1) and IRF1 small interfering RNA (siIRF1). Transfection efficiency was validated using qRT-PCR and Western blotting (Fig. S1C). Subsequently, TNF- α was added to stimulate chondrocytes, and changes in GBP5 gene and protein expression were examined. The results showed that the expression of GBP5 increased after IRF1 overexpression and decreased after IRF1 knockout, regardless of whether TNF- α or PBS was used for stimulation (Fig. 6A and B). Co-transfection experiments with IRF1-overexpressed chondrocytes and specific luciferase reporter plasmids from the GBP5 promoter regions confirmed that IRF1 activated GBP5 transcription. Luciferase reporter vector (pGL3-basic) (Fig. S2C) assays showed significantly higher Firefly/Renilla fluorescence ratios in the WT group after the addition of the IRF1 plasmid, while no significant change occurred in the MUT group (Fig. 6C). ChIP assay results further confirmed the direct binding of IRF1 to the GBP5 promoter regions (Fig. 6D and Fig. S2D). In summary, these findings suggested that IRF1 directly binds to the GBP5 promoter and activates it in chondrocytes.

3.5. IRF1 promotes the pyroptosis of chondrocytes by activating the NLRP3 signaling pathway

To investigate whether IRF1 is involved in ECM synthesis and degradation during the inflammatory response in OA, IRF1 was overexpressed or knocked out in primary chondrocytes, followed by TNF- α stimulation. Markers related to ECM synthesis and degradation were assessed. Results demonstrated that MMP9 and MMP13 gene and protein expression significantly increased after IRF1 overexpression, while COL2A1 and aggrecan expression decreased, consistent with previous findings. Conversely, after IRF1 knockout, MMP9 and MMP13 expression decreased, while COL2A1 and aggrecan expression increased (Fig. 7A and B and Figs. S3A and B). These results confirmed that IRF1 plays a role in the inflammatory response in OA, inhibiting ECM synthesis and promoting degradation.

To determine whether IRF1 can induce chondrocyte pyroptosis by activating the NLRP3 pathway, markers related to the NLRP3 pathway and pyroptosis were assessed. Results showed that NLRP3, Caspase1, GSDMD, pro-IL-1 β , and pro-Caspase1 expression increased after IRF1 overexpression but decreased after IRF1 knockout. These changes were observed even in the PBS-treated cell group and primary human chondrocytes (Fig. 7C, D and Fig. S3B, Figs. S4C and D). Flow cytometry analysis demonstrated that IRF1 positively regulated Caspase1 (Figs. S3C and S3E), and ELISA results showed a positive correlation between IRF1 and the levels of IL-1 β and IL-18 (Figs. S3D and S3F). The same results were obtained when IRF1 was knocked down in primary human chondrocytes (Fig. S4B).

To further illustrate the role of the IRF1/GBP5 axis in promoting chondrocyte pyroptosis, primary mouse chondrocytes were co-transfected with ad-IRF1 and siGBP5. Overexpression of IRF1 increased the expression of pyroptosis-related genes, while co-transfection of ad-IRF1 and siGBP5 significantly decreased their expression (Fig. 7E). In summary, these results indicated that the IRF1/GBP5 axis promotes chondrocyte pyroptosis and ECM degradation by activating the NLRP3 inflammasome, contributing to the development of OA.

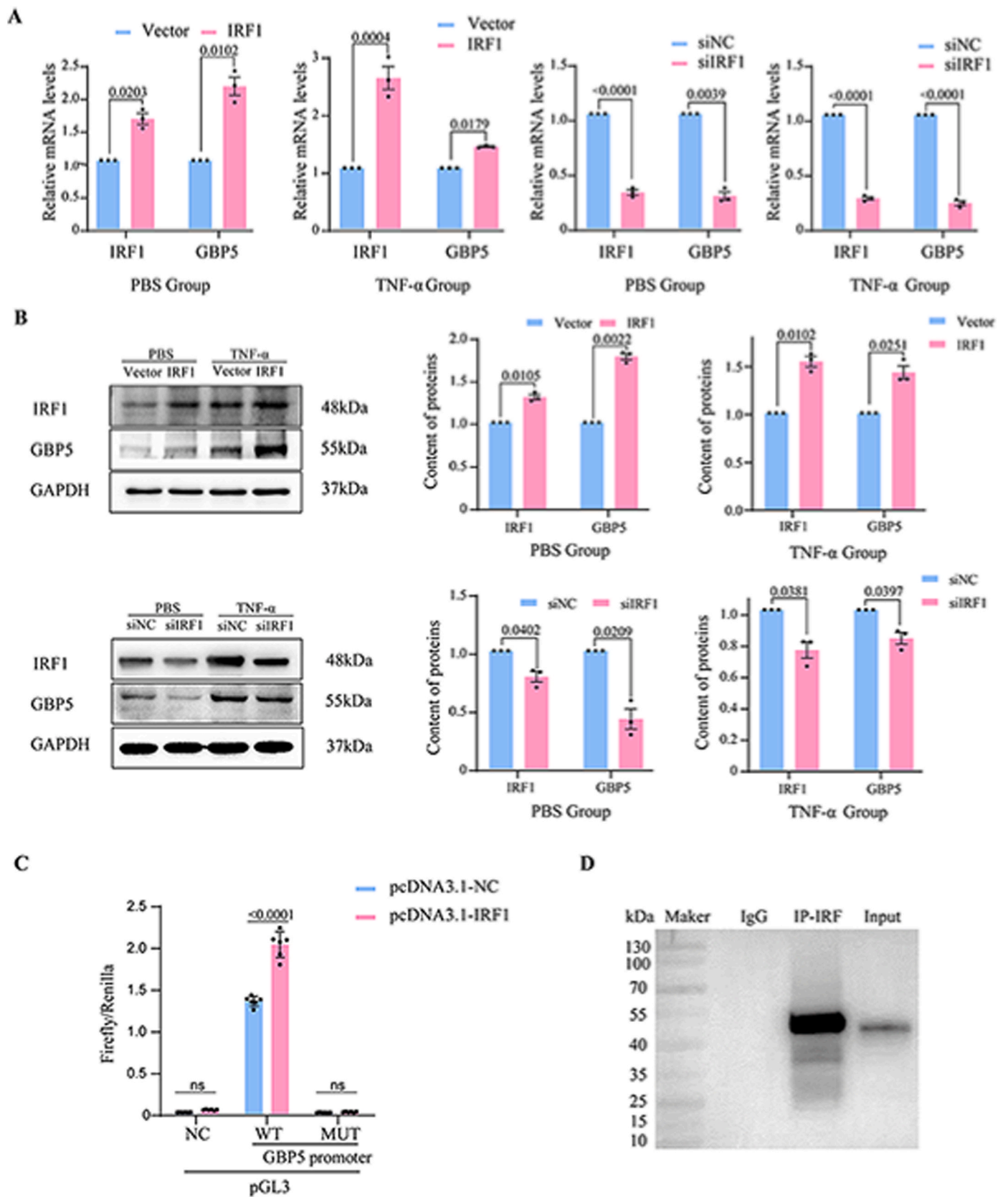
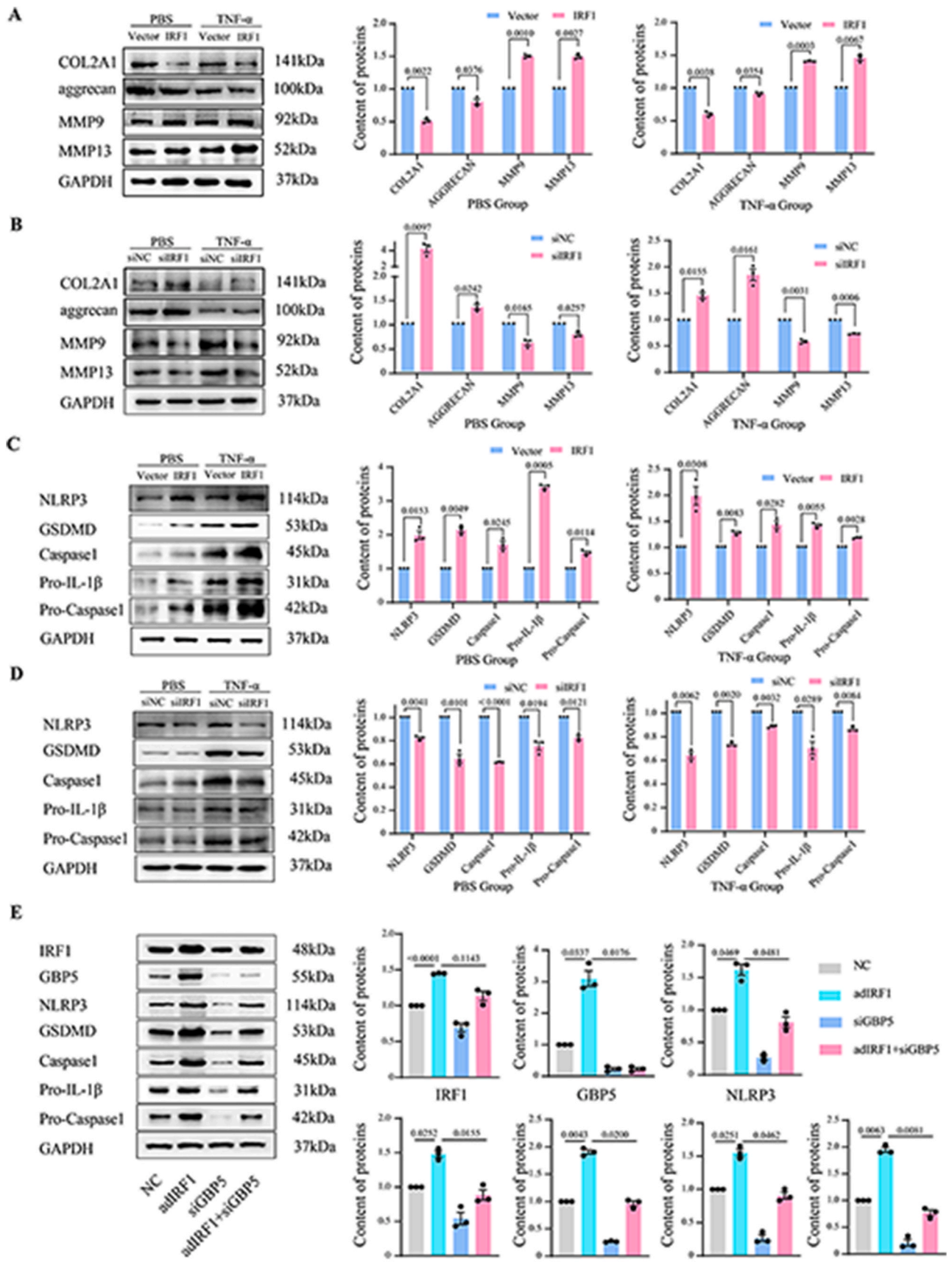


Figure 6. IRF1 bound to the GBP5 promoter region and enhanced its expression (A) The level of expression of the IRF1 and GBP5 genes was determined by RT-qPCR (B) The level of expression of the IRF1 and GBP5 proteins was determined by Western blotting (C) Quantitative statistics of the ratio of Firefly to Renilla in 293 F T cells after adding IRF1 or NC to a dual luciferase reporter gene system containing the wild-type or mutant GBP5 promoter region (D) A ChIP assay for the binding of IRF1 to the promoter region of the GBP5 gene. Two-tailed t-tests were performed to analyze the data on the PBS and TNF- α groups. The data were expressed as the mean \pm SEM.



(caption on next page)

Figure 7. IRF1 promoted the pyroptosis of chondrocytes by activating the NLRP3 signaling pathway (A) The level of expression of the COL2A1, aggrecan, MMP9, and MMP13 proteins C was determined by Western blotting (B) The level of expression of the COL2A1, aggrecan, MMP9, and MMP13 proteins after knocking down IRF1 was determined by Western blotting (C) The level of expression of the NLRP3, Caspase1, GSDMD, Pro-IL-1 β and Pro-Caspase1 proteins after overexpressing IRF1 was determined by Western blotting (D) The level of expression of the NLRP3, Caspase1, GSDMD, Pro-IL-1 β and Pro-Caspase1 proteins after knocking down IRF1 was determined by Western blotting (E) The level of expression of the NLRP3, Caspase1, GSDMD, Pro-IL-1 β and Pro-Caspase1 proteins was determined after cotransfection of ad-IRF1 and siGBP5 by Western blotting. Two-tailed t-tests were performed to analyze the data on the PBS and TNF- α groups. The data were expressed as the mean \pm SEM.

4. Discussion

OA is a significant global health concern; however, the pathogenesis of OA remains unclear. Previous studies have indicated that chondrocyte dysfunction and the loss of ECM are the primary causes of OA [24–26]. Pyroptosis is a form of programmed cell death that leads to the release of numerous inflammatory factors, further exacerbating the destruction of cartilage tissue. The distinctive biochemical and biomechanical properties of the ECM are crucial for the cartilage tissue's functionality. Changes in the composition and damage to the integrity of the ECM can worsen OA [27]. Additionally, chondrocytes are vital for the synthesis and secretion of the ECM. Consequently, chondrocyte death results in detrimental alterations in the articular cartilage's structure [28]. In this study, we demonstrated that GBP5 could promote OA progression through *in vivo* and *in vitro* experiments. This mechanism involves the IRF1/GBP5 axis, which promotes NLRP3 inflammasome activation. The NLRP3 inflammasome induces chondrocyte pyroptosis and enhances cartilage matrix degradation; thus, promoting OA development.

Our findings were consistent with prior studies, further affirming that the balance between cartilage matrix synthesis and degradation influences the occurrence and progression of OA. Our *in vitro* investigations revealed that GBP5 promotes ECM degradation and exacerbates OA by upregulating MMP9 and MMP13 expression while simultaneously reducing COL2A1 and aggrecan expression. ECM homeostasis significantly impacts OA development, with COL2A1 and aggrecan serving as key ECM components playing pivotal roles in OA development. Some studies have elucidated the role of matrix metalloproteinases in OA pathogenesis [29], with MMP9 and MMP13 having specific functions [30–32]. These findings suggest that the effect of GBP5 on cartilage degradation warrants further exploration.

Additional experiments revealed that GBP5 could worsen OA by triggering chondrocyte pyroptosis. Several studies have investigated pyroptosis' role in the development of various diseases, particularly inflammatory conditions. For instance, pyroptosis in hepatocytes after NLRP3 inflammasome activation was found to amplify hepatocyte fibrosis [33]. Similarly, enhancing pyroptosis intensified acute kidney injury through the TNF- α /HMGB1 inflammation signaling pathway activation [34]. GSDMD-mediated cardiomyocyte pyroptosis was identified as a critical event in myocardial ischemia/reperfusion injury [35]. Chondrocyte pyroptosis has also been observed in OA and can be inhibited by miR-140–5p targeting CTSB/NLRP3, which can mitigate cartilage injury in OA [36]. Another study indicated that injured chondrocytes in OA undergo morphological changes due to pyroptosis, underscoring contribution of chondrosis in OA pathology [37].

However, unlike previous studies, our investigation explored GBP5's role in pyroptosis and cartilage dysfunction in OA at the molecular level through *in vivo* and *in vitro* experiments. Pyroptosis is a form of programmed cell death associated with inflammation and can be triggered by various caspases and inflammasome pathways. GSDME cleavage by caspase-3 at its linker generates a GSDME-N fragment that perforates membranes, inducing pyroptosis [38]. Additionally, pyroptosis can be induced by mouse caspase-11 or human caspase-4 and caspase-5, facilitating cytosolic lipopolysaccharide (LPS) and cleavage of the pore-forming protein GSDMD [39]. A previously unknown molecular interaction between AIM2, pyrin, and ZBP1 was found, which promotes inflammatory cell death, including pyroptosis, apoptosis, and necroptosis [40]. Our study examined relevant markers such as NLRP3, Caspase1, GSDMD, Pro-Caspase1, and Pro-IL-1 β , demonstrating that

GBP5 in chondrocytes activated the NLRP3 inflammasome, promoting pyroptosis and worsening OA.

The GBP5 protein is a crucial member of the GTPase family, with its aberrant expression linked to the development of several diseases. The GBP5/NLRP3 inflammasome axis inhibits chemotherapy-induced phlebitis [41] and exacerbates skin inflammation by inducing M1 macrophage polarization via the NF- κ B signaling pathway [42]. In our study, GBP5 was significantly elevated not only in TNF- α -treated chondrocytes but also in the knee joint cartilage of DMM mice and cartilage tissue of humans with OA. Overexpressing GBP5 markedly accelerated chondrocyte pyroptosis and ECM degradation in both PBS-induced and TNF- α -induced chondrocytes, suggesting a causal relationship between GBP5 and chondrocyte pyroptosis in OA at the transcriptional level. Nevertheless, our findings require further confirmation in GBP5-deficient transgenic animals.

Several studies have demonstrated that OA development is regulated by various transcription factors and cytokines [43,44]. Therefore, we further investigated the interaction between IRF1 and GBP5 in OA. Interferon regulatory factor 1 (IRF1), the first identified factor in the IRF family, plays an essential role in tumor prevention, host defense against pathogens, and the inflammatory response [45–47]. Some studies have shown that HS-Cf can inhibit TNF- α -induced IRF1 in porcine chondrocytes, potentially aiding OA treatment [48]. Many studies have reported that IRF1 plays a key role in activating inflammasomes [23]. IRF1 and IRF2 can regulate non-canonical inflammasomes and cause pyroptosis [49]. Another study suggested that IRF1 might control the activation of the NLRP3 inflammasome by affecting mitochondrial DNA replication [50]. Hence, we postulated that IRF1 may be involved in the development of OA through the activation of inflammasomes. Furthermore, IRF1 has been shown to increase the expression of GBPs during Francisella infection, thereby inducing AIM2 inflammasome activation [51]. Notably, the transient overexpression of IRF1 cDNA in mouse fibroblasts leads to a significant elevation in the expression of the Gbp promoter [52]. Given these aforementioned findings, we hypothesized that the IRF1/GBP5 axis can trigger inflammasome activation and promote pyroptosis in chondrocytes, thereby playing a pivotal role in the development of OA. Importantly, it has been verified that IRF1 binds to the promoter region of GBP5 through double luciferase assays and ChIP assays. The results from RT-qPCR and Western blotting analyses corroborated that IRF1 enhances GBP5 expression, consistent with prior research findings. These results suggest that targeting the IRF1/GBP5 axis may hold promise as a therapeutic approach for the treatment of OA.

Author contributions

Hao Tang, Xiaoshan Gong and Shiwu Dong conceived and designed the study; Hao Tang, Xiaoshan Gong, Jingjin Dai, Jun Gu, Zhaoyang Hu and Zicai Dong performed the experiments; Hao Tang, Yuan Xu, Chunrong Zhao, Jiezhong Deng analysed the data; Hao Tang, Xiaoshan Gong and Shiwu Dong wrote and revised the manuscript.

Declaration of competing interest

The authors declare that they have no known competing financial interests or personal relationships that could have appeared to influence the work reported in this paper.

Acknowledgments

This work was supported by grants from Key Program of Natural Science Foundation of China (81930067), the Integration Project of NSFC Joint Fund for Regional Innovation and Development (U23A6008) and the Youth Cultivation Project of Army Medical University (2022XQN07).

Appendix A. Supplementary data

Supplementary data to this article can be found online at <https://doi.org/10.1016/j.jot.2023.11.005>.

References

- Wen C, Xiao G. Advances in osteoarthritis research in 2021 and beyond. *J Orthop Translat* 2022;32:A1–2.
- Zeng C, Li YS, Lei GH. Synovitis in knee osteoarthritis: a precursor or a concomitant feature? *Ann Rheum Dis* 2015;74(10):e58.
- Guo Q, Chen X, Chen J, Zheng G, Xie CL, Wu HQ, et al. STING promotes senescence, apoptosis, and ECM degradation in osteoarthritis via the NF- κ B signaling pathway. *Cell Death Dis* 2021;12(1):13.
- Robinson WH, Lepus CM, Wang Q, Raghu H, Mao R, Lindstrom TM, et al. Low-grade inflammation as a key mediator of the pathogenesis of osteoarthritis. *Nat Rev Rheumatol* 2016;12(10):580–92.
- Musumeci G, Aiello FC, Szychlińska MA, Di Rosa M, Castrogiovanni P, Mobasher A. Osteoarthritis in the XXI century: risk factors and behaviours that influence disease onset and progression. *Int J Mol Sci* 2015;16(3):6093–112.
- Molnar V, Matišić V, Kodvanj I, Bjelica R, Jeleč Ž, Hudetz D, et al. Cytokines and chemokines involved in osteoarthritis pathogenesis. *Int J Mol Sci* 2021;22(17):9208.
- Rim YA, Nam Y, Ju JH. The role of chondrocyte hypertrophy and senescence in osteoarthritis initiation and progression. *Int J Mol Sci* 2020;21(7):2358.
- Yang J, Hu S, Bian Y, Yao J, Wang D, Liu X, et al. Targeting cell death: pyroptosis, ferroptosis, apoptosis and necroptosis in osteoarthritis. *Front Cell Dev Biol* 2022;9:789948.
- Aglietti RA, Dueber EC. Recent insights into the molecular mechanisms underlying pyroptosis and gasdermin family functions. *Trends Immunol* 2017;38(4):261–71.
- Yu P, Zhang X, Liu N, Tang L, Peng C, Chen X. Pyroptosis: mechanisms and diseases. *Signal Transduct Targeted Ther* 2021;6(1):128.
- Zhaolin Z, Guohua L, Shiyuan W, Zuo W. Role of pyroptosis in cardiovascular disease. *Cell Prolif* 2019;52(2):e12563.
- Sordi MB, Magini R de S, Panahipour L, Gruber R. Pyroptosis-mediated periodontal disease. *Int J Mol Sci* 2021;23(1):372.
- Wu J, Lin S, Wan B, Velani B, Zhu Y. Pyroptosis in liver disease: new insights into disease mechanisms. *Aging Dis* 2019;10(5):1094–108.
- Jia S, Yang Y, Bai Y, Wei Y, Zhang H, Tian W, et al. Mechanical stimulation protects against chondrocyte pyroptosis through irisin-induced suppression of PI3K/akt/NF- κ B signal pathway in osteoarthritis. *Front Cell Dev Biol* 2022;10:797855.
- Yu H, Yao S, Zhou C, Fu F, Luo H, Du W, et al. Morroniside attenuates apoptosis and pyroptosis of chondrocytes and ameliorates osteoarthritic development by inhibiting NF- κ B signaling. *J Ethnopharmacol* 2021;266:113447.
- Tong L, Yu H, Huang X, Shen J, Xiao G, Chen L, et al. Current understanding of osteoarthritis pathogenesis and relevant new approaches. *Bone Res* 2022;10(1):60.
- Fujiwara Y, Hizukuri Y, Yamashiro K, Makita N, Ohnishi K, Takeya M, et al. Guanylate-binding protein 5 is a marker of interferon- γ -induced classically activated macrophages. *Clin Transl Immunol* 2016;5(11):e111.
- Shenoy AR, Wellington DA, Kumar P, Kassa H, Booth CJ, Cresswell P, et al. GBP5 promotes NLRP3 inflammasome assembly and immunity in mammals. *Science* 2012;336(6080):481–5.
- Guo H, Ni M, Xu J, Chen F, Yao Z, Yao Y, et al. Transcriptional enhancement of GBP-5 by BATF aggravates sepsis-associated liver injury via NLRP3 inflammasome activation. *Faseb J* 2021;35(6):e21672.
- Haque M, Singh AK, Ouseph MM, Ahmed S. Regulation of synovial inflammation and tissue destruction by guanylate binding protein 5 in synovial fibroblasts from patients with rheumatoid arthritis and rats with adjuvant-induced arthritis. *Arthritis Rheumatol* 2021;73(6):943–54.
- Li Y, Lin X, Wang W, Wang W, Cheng S, Huang Y, et al. The proinflammatory role of guanylate-binding protein 5 in inflammatory bowel diseases. *Front Microbiol* 2022;13:926915.
- Pertea M, Pertea GM, Antonescu CM, Chang TC, Mendell JT, Salzberg SL. StringTie enables improved reconstruction of a transcriptome from RNA-seq reads. *Nat Biotechnol* 2015;33(3):290–5.
- Kuriakose T, Zheng M, Neale G, Kanneganti TD. IRF1 is a transcriptional regulator of ZBP1 promoting NLRP3 inflammasome activation and cell death during influenza virus infection. *J Immunol* 2018;200(4):1489–95.
- Yao X, Sun K, Yu S, Luo J, Guo J, Lin J, et al. Chondrocyte ferroptosis contribute to the progression of osteoarthritis. *J Orthop Translat* 2020;27:33–43.
- Hodgkinson T, Kelly DC, Curtin CM, O'Brien FJ. Mechanosignalling in cartilage: an emerging target for the treatment of osteoarthritis. *Nat Rev Rheumatol* 2022;18(2):67–84.
- van der Kraan PM, van den Berg Western blotting. Chondrocyte hypertrophy and osteoarthritis: role in initiation and progression of cartilage degeneration? *Osteoarthritis Cartilage* 2012;20(3):223–32.
- Peng Z, Sun H, Bumpetch V, Koh Y, Wen Y, Wu D, et al. The regulation of cartilage extracellular matrix homeostasis in joint cartilage degeneration and regeneration. *Biomaterials* 2021;268:120555.
- Hwang HS, Kim HA. Chondrocyte apoptosis in the pathogenesis of osteoarthritis. *Int J Mol Sci* 2015;16(11):26035–54.
- Mehana E-SE, Khafaga AF, El-Blehi SS. The role of matrix metalloproteinases in osteoarthritis pathogenesis: an updated review. *Life Sci* 2019;234:116786.
- Bollmann M, Pinno K, Ehnold LI, Märten N, Märton A, Pap T, et al. MMP-9 mediated Syndecan-4 shedding correlates with osteoarthritis severity. *Osteoarthritis Cartilage* 2021;29(2):280–9.
- Li S, Wang H, Zhang Y, Qiao R, Xia P, Kong Z, et al. COL3A1 and MMP9 serve as potential diagnostic biomarkers of osteoarthritis and are associated with immune cell infiltration. *Front Genet* 2021;12:721258.
- Hu Q, Ecker M. Overview of MMP-13 as a promising target for the treatment of osteoarthritis. *Int J Mol Sci* 2021;22(4):1742.
- Gaul S, Leszczynska A, Alegre F, Kaufmann B, Johnson CD, Adams LA, et al. Hepatocyte pyroptosis and release of inflammasome particles induce stellate cell activation and liver fibrosis. *J Hepatol* 2021;74(1):156–67.
- Wang Y, Zhang H, Chen Q, Jiao F, Shi C, Pei M, et al. TNF- α /HMGB1 inflammation signalling pathway regulates pyroptosis during liver failure and acute kidney injury. *Cell Prolif* 2020;53(6):e12829.
- Shi H, Gao Y, Dong Z, Yang J, Gao R, Li X, et al. GSDMD-mediated cardiomyocyte pyroptosis promotes myocardial I/R injury. *Circ Res* 2021;129(3):383–96.
- Zhang L, Qiu J, Shi J, Liu S, Zou H. MicroRNA-140-5p represses chondrocyte pyroptosis and relieves cartilage injury in osteoarthritis by inhibiting cathepsin B/Nod-like receptor protein 3. *Bioengineered* 2021;12(2):9949–64.
- An S, Hu H, Li Y, Hu Y. Pyroptosis plays a role in osteoarthritis. *Aging Dis* 2020;11(5):1146–57.
- Wang Y, Gao W, Shi X, Ding J, Liu W, He H, et al. Chemotherapy drugs induce pyroptosis through caspase-3 cleavage of a gasdermin. *Nature* 2017;547(7661):99–103.
- Li Z, Liu W, Fu J, Cheng S, Xu Y, Wang Z, et al. Shigella evades pyroptosis by arginine ADP-ribosylation of caspase-11. *Nature* 2021;599(7884):290–5.
- Lee S, Karki R, Wang Y, Nguyen LN, Kalathur RC, Kanneganti TD. AIM2 forms a complex with pyrin and ZBP1 to drive PANoptosis and host defence. *Nature* 2021;597(7876):415–9.
- Liu P, Ye L, Ren Y, Zhao G, Zhang Y, Lu S, et al. Chemotherapy-induced plebitis via the GBP5/NLRP3 inflammasome axis and the therapeutic effect of aescin. *Br J Pharmacol* 2023;180(8):1132–47.
- Zhou L, Zhao H, Zhao H, Meng X, Zhao Z, Xie H, et al. GBP5 exacerbates rosacea-like skin inflammation by skewing macrophage polarization towards M1 phenotype through the NF- κ B signalling pathway. *J Eur Acad Dermatol Venereol* 2023;37(4):796–809.
- Hu W, Chen Y, Dou C, Dong S. Microenvironment in subchondral bone: predominant regulator for the treatment of osteoarthritis. *Ann Rheum Dis* 2021;80(4):413–22.
- Hu Y, Wang L, Zhao Z, Lu W, Fan J, Gao B, et al. Cytokines CCL2 and CXCL1 be potential novel predictors of early bone loss. *Mol Med Rep* 2020;22(6):4716–24.
- Zhou H, Tang YD, Zheng C. Revisiting IRF1-mediated antiviral innate immunity. *Cytokine Growth Factor Rev* 2022;64:1–6.
- Harikumar KB, Yester JW, Surace MJ, Oyeniran C, Price MM, Huang WC, et al. K63-linked polyubiquitination of transcription factor IRF1 is essential for IL-1-induced production of chemokines CXCL10 and CCL5. *Nat Immunol* 2014;15(3):231–8.
- Buccione C, Fragale A, Polverino F, Zicchettu G, Aricò E, Belardelli F, et al. Role of interferon regulatory factor 1 in governing Treg depletion, Th1 polarization, inflammasome activation and antitumor efficacy of cyclophosphamide. *Int J Cancer* 2018;142(5):976–87.
- Liu FC, Huang HS, Huang CY, Yang R, Chang DM, Lai JH, et al. A benzamide-linked small molecule HS-Cf inhibits TNF- α -induced interferon regulatory factor-1 in porcine chondrocytes: a potential disease-modifying drug for osteoarthritis therapeutics. *J Clin Immunol* 2011;31(6):1131–42.
- Thygesen SJ, Stacey KJ. IRF1 and IRF2 regulate the non-canonical inflammasome. *EMBO Rep* 2019;20(9):e48891.
- Zhong Z, Liang S, Sanchez-Lopez E, He F, Shalpour S, Lin XJ, et al. New mitochondrial DNA synthesis enables NLRP3 inflammasome activation. *Nature* 2018;560(7717):198–203.
- Man SM, Karki R, Malireddi RKS, Neale G, Vogel P, Yamamoto M, et al. The transcription factor IRF1 and guanylate-binding proteins target activation of the AIM2 inflammasome by Francisella infection. *Nat Immunol* 2015;16(5):467–75.
- Briken V, Ruffner H, Schultz U, Schwarz A, Reis LF, Strehlow I, et al. Interferon regulatory factor 1 is required for mouse Gbp gene activation by gamma interferon. *Mol Cell Biol* 1995;15(2):975–82.